ACADEMIA ROMÂNĂ
Revue Roumaine de Chimie
https://www.icf.ro/rrch/

Rev. Roum. Chim.,
2024, *69*(1–2), 49–56
DOI: 10.33224/rrch.2024.69.1-2.06

PREPARATION, STRUCTURE AND PROPERTIES OF A NOVEL ONE-DIMENSIONAL ERBIUM (III) COMPLEX

Ting PENG,[a,b] Xiao-Yong CHEN,[a,c] Ting-Qun QIU,[a] Jia-Liang FAN,[a,b] Li-Yong HUANG,[a,d] Xiu-Guang YI[a,*] and Xu-Liang NIE[f,*]

[a]School of Chemistry and Chemical Engineering, Jinggangshan University, Ji'an, Jiangxi Province, 343009, China
[b]Ji'an Central People's Hospital, Ji'an, Jiangxi Province, 343000, China
[c]Ji'an No. 1 Middle School, Ji'an, Jiangxi Province, 343000,China
[d]Jiangxi Hongqiao New Energy Technology Co., LTD., Xinyu, Jiangxi Province, 338000, China
[f]College of Chemistry & Materials, Jiangxi Agricultural University, Nanchang 330045, China

Received July 11, 2023

A novel one-dimensional erbium complex [ErL2(NO3)(H2O)2]n (HL = 2-picolinic acid) was synthesized by hydrothermal methods, and its crystal structure was determined by single crystal x-ray diffraction. The complex crystallize in monoclinic system, space group C2/c with a = 15.7525(5) Å, b = 11.4958(4) Å, c = 9.7977(3) Å, β = 102.862(3) º, V = 1729.72(10) Å3, C12H10ErN3O9, Mr = 507.49, Z = 4, Dc = 1.949 g·cm^{-3}, F(000) = 972, μ = 4.901 mm^{-1}, S = 1.119, λ(MoKα) = 0.071073 nm, R = 0.0239 and wR = 0.0668. The 2-picolinic acid ligand adopts bidentate bridging coordination mode to connect adjacent erbium ions to form a one-dimensional chain structure. A series of properties of the complex were measured by solid-state photoluminescence, solid-state diffuse reflection and differential scanning calorimetry.

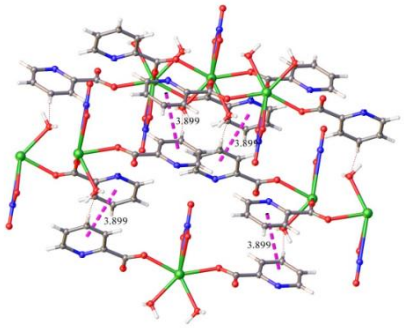

INTRODUCTION

In the past decade, inorganic and organic hybrid complexes have attracted great attention because of their chemical and physical properties and many potential applications, such as catalysis, gas storage and separation, sensors, lithium-ion batteries, magnetic and optical properties.[1–5] Why are inorganic and organic hybrid complexes always the focus of chemist and materialists? Obviously, because there metal ions and organic ligands have super coordination ability and a variety of coordination modes, there are many types, especially metal rare earth elements and organic ligands containing carboxylic acids.[6–10]

In the design and preparation of complexes, it is very important to choose a good ligand. As a good flexible ligand carboxyl group, it not only has a variety of coordination modes, such as single tooth coordination, symmetrical chelation coordination, asymmetric chelation coordination, single oxygen bridging coordination, oxygen bridging coordination and so on, but also has strong coordination ability.[11–15] The properties of rare earth

* Corresponding authors: jayxgggchem@163.com ; niexuliang1981@163.com

compounds are mainly due to the abundance of 4*f* electrons in lanthanide ions. In general, rare earth compounds can show that if the transition electrons of 4*f* can occur effectively, but 4*f* electrons are actually difficult to appear because of low absorption coefficient of rare earth ions. Therefore, it is difficult to obtain ideal photoluminescence emission.[16–18]

In order to achieve strong photoluminescence, novel rare earth compounds are usually designed and prepared by using organic ligands with conjugated motifs, such as heterocyclic derivatives and aromatic carboxylic acids. The organic ligands can be use containing appropriate chromophores in lanthanide complexes. The strongly sbsorb light in the UV region and transfer the excitation energy from the ligands to the lanthanide ions via an antenna effect. Results, Ln(III) complexes emits strongly characteristic luminescence.

Generally, the methods of crystal preparation include hydrothermal method, chemical vapor condensation method and solid state method. Among these methods, hydrothermal method refers to an effective method for inorganic synthesis and material treatment by using solvent as the reaction system in a special closed space environment (higt-rpessure reactor), heating and rpesurizing the reaction system to create a relatively high temperature and high pressure reaction environment, so that some insoluble or insoluble reactants can be dissolved and recrystallized.

The author Research team recently gets much interest in studying the crystal structures and physicochemical properties of novel lanthanide compounds. In the present work, a novel erbium complex $[Er_2L_2(NO_3)_4(H_2O)_2]n$ (**1**) is synthesized. According to the electronic transition form and fluorescence characteristics of the luminescence of rare earth complexes, the erbium complexes exhibit weak rare earth ion fluorescene and weak ligand fluorescence and phosphorescence. The energy level difference between the lowest excited state and the ground state of the group of rare earth ion is small, the non-radiative transition probability is large, and the emission is in the near infrared region. In this work, the crystal structure, photoluminescence charecteristics and energy gap band of the complex were analyzed.

EXPERIMENTAL

Materials and Instrumentation

All reagents and chemicals were reagent grade, commercially available and directly applied for the reaction. Infrared spectra was obtained by using KBr disk with a PE Spectrum-One FT-IR spectrometer. Solid-state UV/Visible Diffuse Reflectance spectroscopy was carried out on a computer-controlled TU1901 UV/Visible spectrometer. Fine ground powder sample were coated on barium sulfate to obtain 100% reflectivity. Photoluminescence characteristics were carried out on F97XP photoluminescence spectrometer.

Synthesis of the title complex (1)

The title complex (**1**) was prepared by mixing $Er(NO_3)_3{\cdot}6H_2O$ (1 mmol, 461.37 mg), 2-picolinic acid (2 mmol, 246 mg) and 10 mL distilled water into a 25 mL Teflon-lined stainless-steel autocalve. The autoclave was heated at 473 K in an oven for 7 days and then powered off. When the autoclave was naturally cooled down to room temperature, pale purple block-like crystals were obtained and used for the collection for single-crystal X-ray data. The yield was 75% based on Erbium. IR peaks (cm^{-1}): 3415 (vs), 1654 (vs), 1598 (vs), 1409 (vs), 1294 (m), 1193 (m), 867 (m), 759 (s), 698 (s), as shown in Fig. 1.

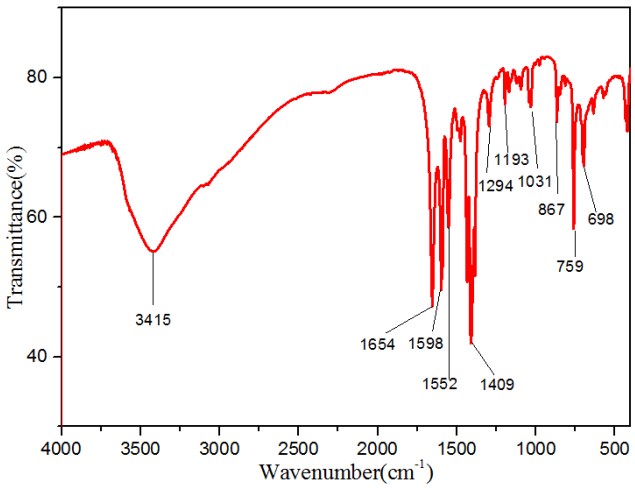

Fig.1 – FTIR spectra of the title complex (1).

X-ray Crystallographic Determination

The diffraction data were collected on a SuperNova CCD X-ray diffractometer using carefully selected single crystals of the title complex. The X-ray source was graphite monochromated Mo-$K\alpha$ (λ = 0.71073 Å) and ω scan method was employed. The reduction and empirical absorption correction of diffraction data were carried out with the crystalClear software. Using Olex2,[19] the structure of the title complex was solved with the ShelXT,[20] the structure solution program using Intrinsic Phasing and refined with the ShelXL[21] refinement package using Least Squares minimization. All of the non-hydrogen atoms were generated based on the subsequent Fourier difference maps and were refined anisotropically. The hydrogen atoms, except for the lattice water, were located theoretically and ride on their parent atoms. Reflections measured are 10864; the final R = 0.0436 for 5254 parameters and 449 observed reflections with $I > 2\sigma(I)$ and wR = 0.1172; index ranges are $-18 \le h \le 18$, $-13 \le k \le 13$, $-11 \le l \le 11$, S = 1.18, $(\Delta\sigma)_{max}$ = 0.841 e/Å^3 and $(\Delta\sigma)_{min}$ = –0.646 e/Å^3. Table 1 provides a summary of the crystallographic data and refinement results. Table 2 lists selected bond lengths and angles for the title complex.

Table 1

Summary of crystal data

Empirical formula	C12 H10 Er N3 O9
Color and Habit	pale purple block
Crystal Size (mm)	0.28 × 0.06 × 0.04
Crystal system	Monoclinic
Space group	*C*2/*c*
a (Å)	15.7525(5)
b (Å)	11.4958(4)
c (Å)	9.7977(3)
α /°	90
β/°	102.862(3)
γ/°	90
Volume(Å ^{3})	1949.72(10)
Z	4
Formula weight	507.49
Density(cal.)(Mg/m^3)	1.949
Absorption coefficient(mm^{-1})	4.901
F(000)	920
Reflections measured	5094
Index ranges of measured data	$-18 \le h \le 19$, $-13 \le k \le 13$, $-11 \le l \le 11$
Independent reflections	1606 (R_{int} = 0.0192)
Observed Reflection	1462 (>2sigma(I))
Parameter/Restraints/Data(obs.)	1606 / 1 / 119
Final *R* indices (obs.)	R_1 = 0.0239, wR_2 = 0.0661
R indices (all)	R_1 = 0.0251, wR_2 = 0.0668
S	1.119
Largest difference peak(e. Å $^{-3}$)	0.920, –0.693

Table 2

Selected bond lengths (Å) and bond angles (°) for the title complex

Distance	(Å)	Distance	(Å)
Er(1)-O(1)	2.219(4)	Er(1)-O(1)^{i}	2.219(4)
Er(1)-O(2)^{ii}	2.331(3)	Er(1)-O(2)^{iii}	2.331(3)
Er(1)-O(3)	2.366(4)	Er(1)-O(3)^{i}	2.366(4)
Er(1)-O(4)	2.445(4)	Er(1)-O(4)^{i}	2.445(4)
Angle	(°)	Angle	(°)
O(1)^{i}-Er(1)-O(1)	159.8(2)	O(1)^{i}-Er(1)-O(2)^{ii}	99.72(13)
O(1)-Er(1)-O(2)^{ii}	86.75(13)	O(1)^{i}-Er(1)-O(2)^{iii}	86.75(13)
O(1)-Er(1)-O(2)^{iii}	99.73(13)	O(2)^{ii}-Er(1)-O(2)^{iii}	142.78(17)
O(1)^{i}-Er(1)-O(3)^{i}	79.36(14)	O(1)-Er(1)-O(3)^{i}	84.05(13)
O(2)^{ii}-Er(1)-O(3)^{i}	74.32(13)	O(2)^{iii}-Er(1)-O(3)^{i}	142.54(13)
O(1)^{i}-Er(1)-O(3)	84.05(13)	O(1)-Er(1)-O(3)	79.36(14)
O(2)^{ii}-Er(1)-O(3)	142.54(13)	O(2)^{iii}-Er(1)-O(3)	74.32(13)
O(3)^{i}-Er(1)-O(3)	69.79(19)	O(1)^{i}-Er(1)-O(4)^{i}	73.85(15)

(*Table 2 continues*)

(*Table 2 continues*)

Angle	(°)	Angle	(°)
O(1)-Er(1)-O(4)^{i}	126.36(15)	O(2)^{ii}-Er(1)-O(4)^{i}	73.81(13)
O(2)^{iii}-Er(1)-O(4)^{i}	72.97(12)	O(3)^{i}-Er(1)-O(4)^{i}	133.62(13)
O(3)-Er(1)-O(4)^{i}	141.20(15)	O(1)^{i}-Er(1)-O(4)	126.36(15)
O(1)-Er(1)-O(4)	73.85(15)	O(2)^{ii}-Er(1)-O(4)	72.97(12)
O(2)^{iii}-Er(1)-O(4)	73.81(13)	O(3)^{i}-Er(1)-O(4)	141.20(15)
O(3)-Er(1)-O(4)	133.62(13)	O(4)^{i}-Er(1)-O(4)	52.8(2)

symmetry codes: i = –*x*+1,*y*,–*z*+1/2 ii = *x*,–*y*,*z*+1/2 iii = –*x*+1,–*y*,–*z*

RESULTS AND DISCUSSION

Crystal Structure

The molecular structure of the title complex (**1**) is shown in Fig. 2. The title complex (**1**) features a one-dimensional (1-D) chain structure is shown in Fig. 3. Single-crystal X-ray diffraction measurement revealed that the title complex (1) is a neutral molecule that crystallizes in the space group *C*2/*c* of the monoclinic system. The Er(1) ion is located at the inversion center and coordinates with four L molecules, one nitrate ion and two water molecules respectively, yielding one slightly deformed hexagonal pyramid geometry. Erbium ions are eight-coordinated, and coordinated to eight oxygen atoms, of which four oxygen atoms are from four L ligands, of which two oxygen atoms are from two coordination water molecules, and two oxygen atoms are from one nitrate ion, respectively. The following bond distances were observed: Er(1)-O(1) 2.219(4) Å, Er(1)-O(2)^{i} 2.331(3) Å, Er(1)-O(3) 2.366(4) Å, Er(1)-O(4)^{iii} 2.445(4) Å. These are equivalent to those reported in the literature.[22–24] The 2-picolinic acid ligand adopts bidentate bridging coordination mode to connect adjacent erbium ions to form a one-dimensional chain structure (Fig. 3).

The distances of Er(1)···Er(1)^{i} is 4.9237(2) Å, and the angles Er(1)···Er(1)^{i}···Er(1)^{ii} is 168.481º. Additionally, in the molecule there is offset face-to-face π···π stacking interaction between *Cg*1···*Cg*1 (symmetry codes: ½–*x*, ½–*y*, –*z*), (*Cg*1 is the ring consisting of C1 to C5, and N1). The centroid-centroid distance of *Cg*1···*Cg*1 is 3.899 Å, with a slippage distance of 1.750 Å and with a dihedral angle of 0 ˚, as shown in Fig. 4. The intramolecular hydrogen bonds can be found between the oxygen atoms (O3-H1···O4; O3-H1···O1). The intermolecular hydrogen bond like C4-H4···O5, as shown in Table 3 and Fig. 4. In the title complex, there are π···π stacking interactions, van der Waals and hydrogen bonds attraction yielding the 3-*D* structure, the crystal packing is presented in Fig. 5.

Table 3

Hydrogen Bond Lengths (Å) and Bond Angles (°)

D-H···A	[ARU]	d(D-H)	d(H-A)	d(D···A)	∠ DHA
O3-H1···O4	[5_655]	0.814(10)	2.36(2)	3.149(6)	162(7)
O3-H1···O1	[5_655]	0.814(10)	2.50(7)	2.986(5)	120(7)
C4-H4···O5	[3_455]	0.93	2.61	3.319(6)	133.8

Symmetry codes: [5_655] = –*x*+1, –*y*, –*z*; [3_455] = *x*–1/2, *y*+1/2, *z*.+

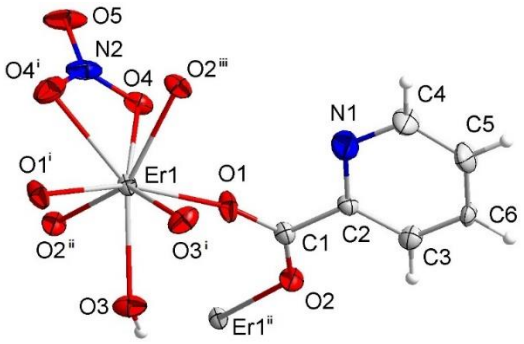

Fig. 2 – The ORTEP drawing of the title complex (**1**); ellipsoids are shown at the 30% probability level.

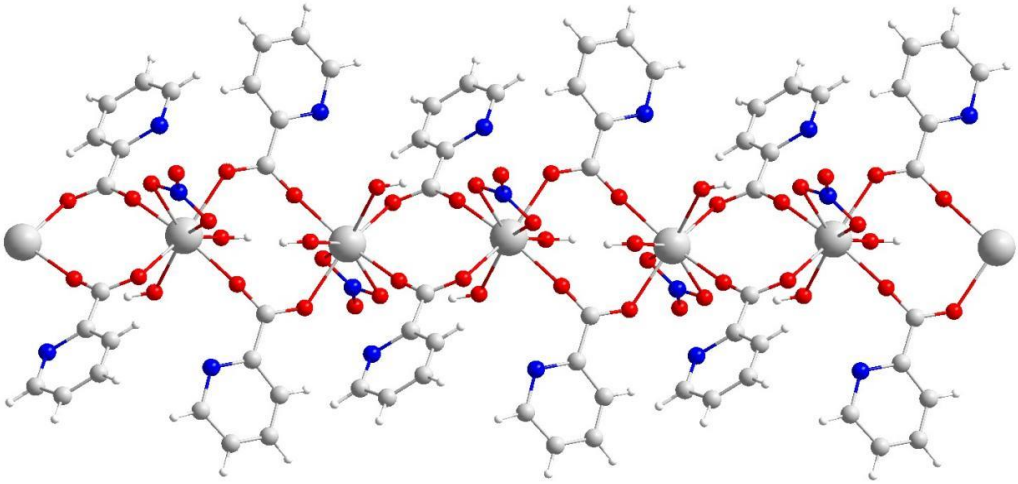

Fig. 3 – The 1-D chain-like structure of the title complex (**1**) viewed along the *c* axis.

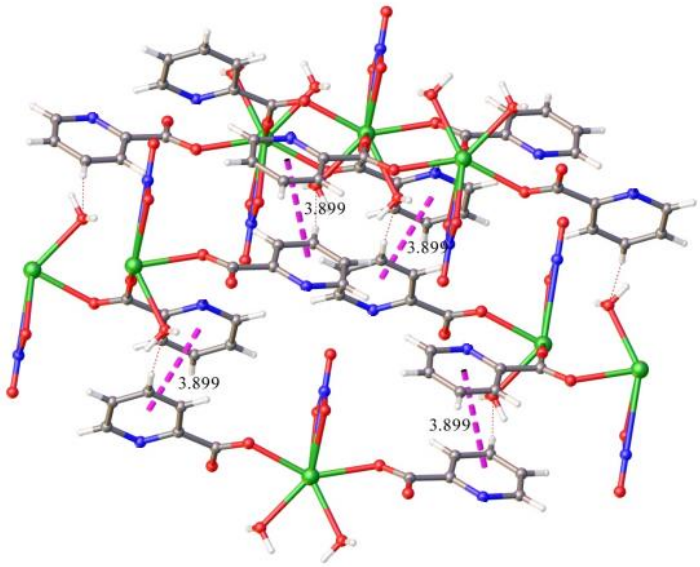

Fig. 4 – The π···π stacking interactions diagram of the title complex (**1**).

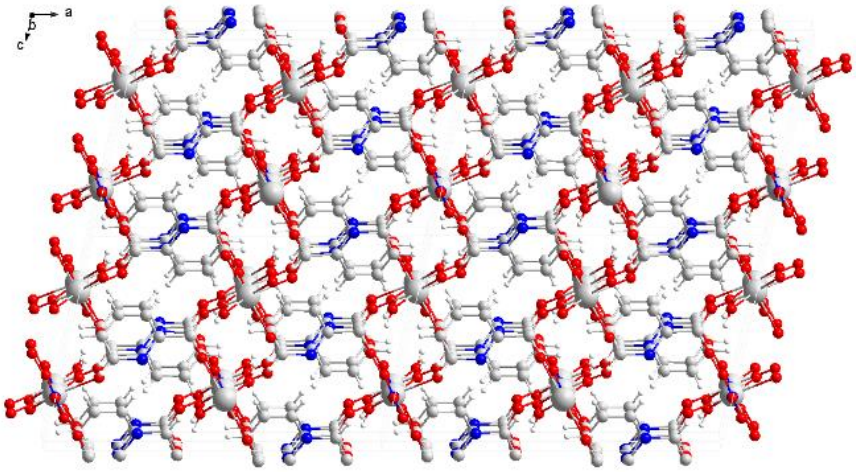

Fig. 5 – The packing diagram of the title complex (**1**) viewed along the *a* axis.

Solid-State UV-Vis Diffuse Reflectance Spectra of the title complex (1)

Based on barium sulfate as the reference for 100% reflectivity, the UV-Vis diffuse reflectance spectra of the title complex (**1**) was measured at room temperature, using the solid-state compound. Date processing adopts $(ahv)^{1/n} = A(hv–E_g)$, which is the famous Tauc plot formula.[25–27] In the $(ahv)^{1/n} = A(hv–E_g)$, where a is the absorption coefficient, h is the Planck's constant (6.63×10^{-34} J·s), v is the frequency, A is the constant and E_g is the band gap of semiconductor. First, the $(ahv)^{1/n}$ ($n = 1/2$) and hv are obtained by using the solid-state UV-Vis diffuse reflectance spectrum, where $hv = hc/\lambda$, λ is the wavelength of light. Second, the graph is draw with $(ahv)^{1/n}$ as the vertical coordinate and hv (1 eV = 1.6×10^{-19} J) as the horizontal coordinate. Finally, the straight part of the figure is extrapolated to the horizontal coordinate, and the intersection point is the energy band gap, as shown in Fig. 6. The title complex (**1**) shows a broad optical energy band gap 3.25 eV. Therefore, this may be a good candidate material for broad band gap semiconductors. The energy band gap of 3.25 eV of the title complex (**1**) is obviously larger than those of GaAs (1.4 eV), CdTe (1.5 eV), and CuInS2 (1.55 eV), which are called efficient band gap photovoltaic materials.[28–30]

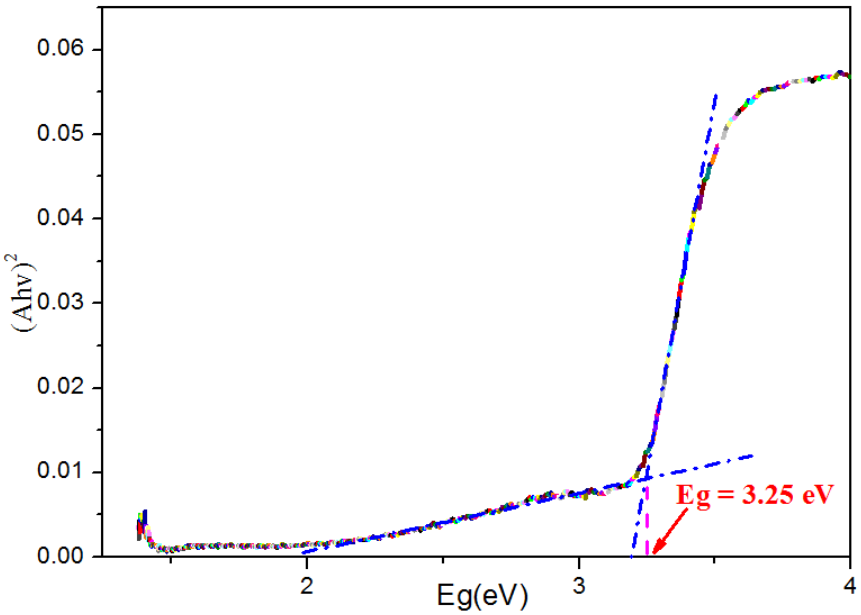

Fig 6 – Solid-State UV-Vis diffuse reflectance Spectra of the title complex (1).

Solid-State Photoluminescence Spectra of the title complex (1)

At the same times, in order to reveal the potential photoluminescence characteristics of the title complex (**1**), the photoluminescence spectra of the solid state samples at room temperature were measured, and the results are shown in Fig. 7. It can be seen that the photoluminescence spectrum of the title complex (**1**) shown that it has an effective absorption in the range of 200–300 nm with two peaks located at 655 nm and 710 nm, which can be ascribed to $^4F_{9/2}\rightarrow{}^4I_{15/2}$ and $^4I_{11/2}\rightarrow{}^4I_{15/2}$, respectively.[31–35] When excited under 264 nm, it exhibits two emission bands in the range of 625–750 nm with the peak values being 655 nm and 710 nm, respectively. The strongest emission band of the title complex (**1**) is in the red light region, so the title complex (**1**) is possibly a red light emitting material. 2-Picolinic acid ligand, as an organic fluorophore, has strong absorption in the ultraviolet region and can effectively transfer energy. When it is at an appropriate distance from the Er(III) ion, it can transfer energy to Er(III) ions, thus sensitizing the luminescence of Er(III) ions. In the title complex, 2-picolinic acid shows the role of energy donor and bonding group. These photoluminescence emission bands can be attributed to the characteristic emission of the 4*f* electrons intrashell transition of the Er^{3+} ion, namely the emission bands at 655 nm and 710 nm can be assigned to the $^4F_{9/2}\rightarrow{}^4I_{15/2}$ and $^4I_{11/2}\rightarrow{}^4I_{15/2}$ ion. The photoluminescence emission peaks are well separated and strong, so the 2-picolinic acid ligand is an ideal "antenna" for Er^{3+} ion.

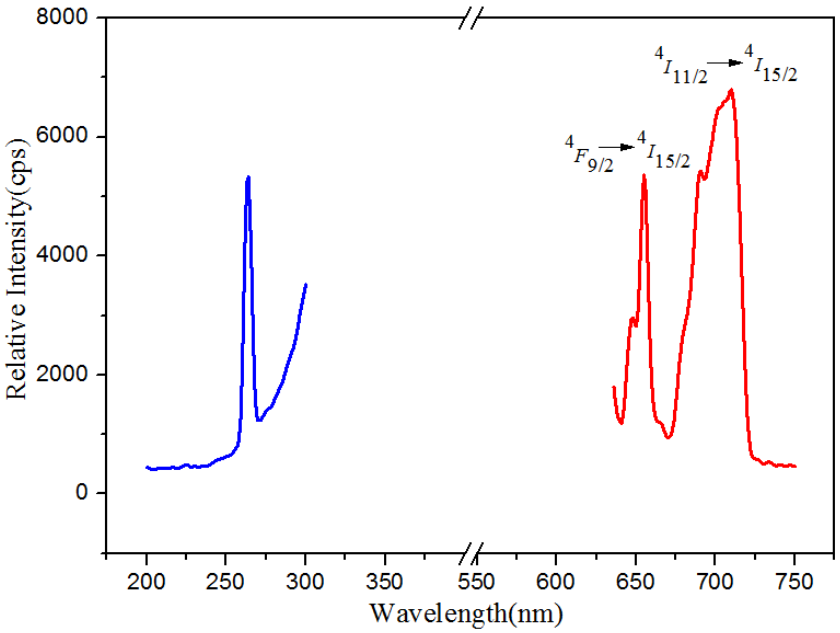

Fig. 7 – Solid-state photoluminescence spectra of the title complex (1) measured at room temperature. Blue – excitation spectra; red – emission spectra.

Differential Scanning Calorimetry (DSC) spectra of the title complex (1)

The DSC is an effective method to study the structural phase transfer of thermal energy caused by molecular swing, one-dimensional chain expansion or frame deformation with the change of external temperature. The title complex (**1**) was tested by DSC under nitrogen protection, 20–300 °C and temperature change rate of 10 K·min^{-1}, as shown in Fig. 8. With the temperature increases gradually from low temperature, an obvious endothermic peak is generated near 198.02 °C. This is because the structure of the title complex (**1**) changes significantly in this temperature range (the collapse of metal organic framework). With the decrease of temperature, the DSC curve does not change significantly, indicating that the title complex (**1**) is an irreversible phase change material.

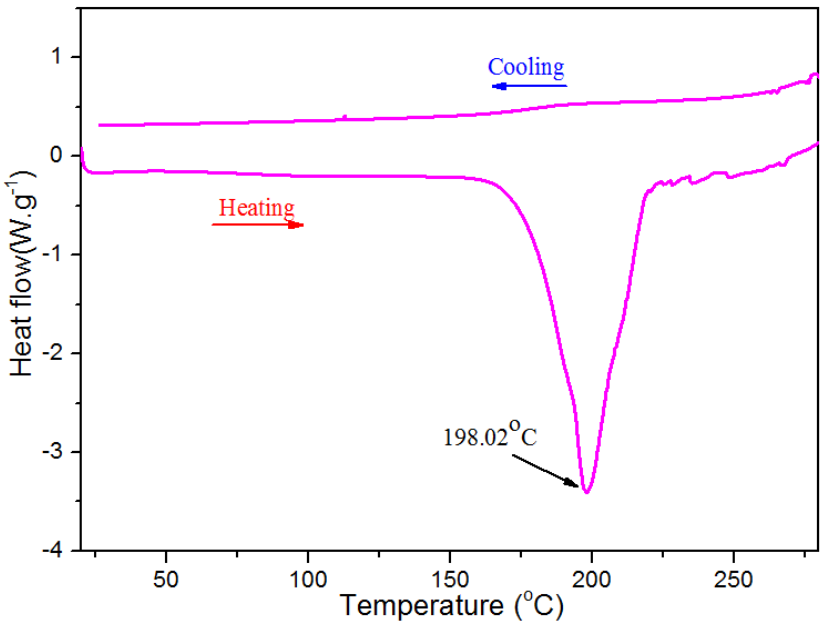

Fig. 8 – The DSC spectra of the title complex (1).

CONCLUSIONS

In summary, a novel erbium (III) complex with 2-picolinic acid (HL) ligand including lattice water has been synthesized and characterized by single-crystal X-ray diffraction. The hexagonal pyramid geometry interconnect together via two HL ligands to form a 1-*D* chain running along the *c* axis and π···π stacking interactions, van der Waals and hydrogen bonds attraction yielding the 3-*D* supramolecular structure. Based on the solid-state photoluminescent spectrum, the solid-state diffuse reflectance spectrum experiment and DSC spectra, we believe that the title complex may be a good red light photoluminescent material, a candidate material for wide band gap semiconductor and an irreversible phase change material. The interest of the research group is to synthesize more metal complexes to reveal the intrinsic relationship among the synthesis methods, crystal structures and properties.

Supplementary Materials. Crystallographic data for the structural analysis have been deposited with the Cambridge Crystallographic Data Center, CCDC No. 2170017. Copies of this information can be obtained free of charge from the Director, CCDC, 12 Union Road, Cambridge, CBZ, 1 EZ, UK (fax: +44-1223-336033); email: deposit@ccdc.cam.ac.uk or online at http://www.ccdc.cam.ac.uk.

Data Availability. Data Availability CCDC 2170017 contain the supplementary crystallographic data for the title complex. The data can be obtained free of charge from the Cambridge Crystallographic Data Centre via www.ccdc.com.ac.uk/structures.

Acknowledgements. The National Natural Science Foundation of China (22168018), Natural Science Foundation of Jiangxi Province of China (20232BAB203048), the Higher Education and Teaching Reform of Jiangxi Education Committee of China (JXJG-22-9-23), the Science and Technology Plan Project of Ji'an (20211-025317), Doctoral Research Startup Foundation of Jinggangshan University (JZB1905).

REFERENCES

1. P. Xu, J. Liu, J. H. Huang, F. Yu, C. H. Li and Y. X. Zheng, *New J. Chem.*, **2021**, *45*, 13168–13174.
2. Y. Abbas, S. N. Yun, M. S. Javed, J. G. Chen, M. F. Tahir, Z. Q. Wang, C. Yang, A. Arshad and S. Hussain, *Ceram. Int.*, **2020**, *46*, 4470–4476.
3. H. H. Chen, X. G. Yi, C. W. Pan, J. W. Wen and C. Zhang, *Chinese J. Struct. Chem.*, **2021**, *40*, 501–506.
4. J. Li, L. S. Shi, X. G. Yi, X. N. Fang, T. Guo and Y. X. Li, *Chinese J. Struct. Chem.*, **2020**, *39*, 551–558.
5. A. Quader, G. M. Mustafa, S. K. Abbas, H. Ahmad and S. Atiq, *Chem. Eng. J.*, **2020**, *396*, 125198–125206.
6. D. Mahmoud, M. S. EI-Deab, M. E. Elshakre and N. K. Allam, *J. Phys. Chem. C*, **2020**, *124*, 7007–7015.
7. J. N. Xing, M. Shu, W. Y. Wang, R. Zhang and J. Liu, *Chinese J. Inorg. Chem.*, **2021**, *37*, 1847–1852.
8. W. A. Fu, H. J. Chen, Y. Y. Han, W. Y. Wang, R. Zhang and J. Liu, *New J. Chem.*, **2021**, *45*, 19082–19087.
9. H. Shi, F. F. Zhao, X. H.Chen, S. L. Yang, J. N. Xing, H. J. Chen, R. Zhang and J. Liu, *Tetrahedron Letters*, **2019**, *60*, 151330–151334.
10. H. J. Chen, G. Y. Lyu, Y. F. Yue, T. W. Wang, D. P. Li, H. Shi, J. N. Xing, J. Y. Shao, R. Zhang, and J. Liu, *J. Mater. Chem. C*, **2019**, *7*, 7249–7259.
11. X. W. Li, N. Ma, G. T. Xu, R. Zhang and J. Liu, *Solar Energ. Mater. Solar Cells*, **2022**, *234*, 111449–111454.
12. C. Jeffrey, R. B. David, L. Li and L. M. David, *J. Biomed. Optics*, **2019**, *24*, 051409–051420.
13. W. Y. Wang, H. J. Chen, Y. F. Yue, R. Zhang and J. Liu, *Dyes and Pigments*, **2021**, *194*, 109615–109622.
14. M. Li, H. P. Wu, S. Zhang, Y. F. Liu, Y. Q. Chen and S. P. Chen, *Chinese J. Inorg. Chem.*, **2022**, *38*, 171–180.
15. J. Su J, S. Yuan, J. Li, H. Y. Wang, J. Y. Ge, H. F. Drake, C. F. Leong, F. Yu, D. M. D'Alessandro, M. Kurmoo, J. L. Zuo and H. C. Zhou, *Chem. Euro. J.*, **2021**, *27*, 622–627.
16. X. G. Yi, Y. Z. Liu, X. N. Fang, X. Y. Zhou, Y. X. Li, *Chinese J. Struct. Chem.*, **2019**, 38, 325–330.
17. C. C. Zhang, X. F. Ma, P. P. Cen, X. Y. Jin, J. H. Yang and Y. Q. Zhang, *Dalton Transactions*, **2020**, *49*, 14123–14132.
18. Y. L. Wang, C. B. Han, Y. Q. Zhang, Q. Y. Liu, C. M. Liu and S. G. Yin, *Inorg. Chem.*, **2016**, *55*, 5578–5584.
19. O. V. Dolomanov, L. J. Bourhis and R. J. Gildea, *J. Appl. Crystall.*, **2009**, *42*, 339–341.
20. G. M. Sheldrick, *Acta Crystall. Section A*, **2008**, *64*, 112–122.
21. G. M. Sheldrick, *Acta Crystall. Section C*, **2015**, *71*, 3–8.
22. K. X. Shang, W. T. He, J. Sun, D. C. Hu and J. C. Liu, *J. Molec. Struct.*, **2021**, *1246*, 131097–131106.
23. L. Spillecke, C. Koo, O. Maximova, V. S. Mironov, V. A. Kopotkov, D. V. Korchagin, A. N. Vasiliev E. B. Yagubskii and R. Klingeler, *Dalton Transactions*, **2021**, 295–304.
24. X. Y. Sun, J. N. Li, G. M. Dong, Y. L.Tao and S. Q. Yang, *J. Iran. Chem. Soc.*, **2021**, *18*, 1303–1309.
25. Y. F. Wang, X. G. Yi, X. N. Fang, J. Li, Y. Xu and S. K. Xie, *Inorg. Nano-Metal Chem.*, **2020**, *50*, 1130–1136.
26. J. Tuac, R. Grigorovici and A. Vancu, *Physica Status Solid (b)*, **1966**, *15*, 627–637.
27. R. Surekha, S. R. Thilagavathy, R. Sagayaraj and R. Ambujam, *Optik*, **2014**, *125*, 934–938.
28. X. N. Fang, X. G. Yi, Z. Q. Yi, J. Y. Chen and Y. X. Li, *Chinese J. Inorg. Chem.*, **2019**, *35*, 930–936.
29. W. S. Lin, H. M. Kuang, H. Luo and W. T. Chen, *Chinese J. Struct. Chem.*, **2019**, *38*, 1012–1020.
30. F. Q. Huang, K. Mitchell and J. A. Ibers, *Inorg. Chem.*, **2001**, *40*, 5123–5126.
31. P. Kostka, I. Kabalci, T. Tay, P. Gladkov and J. Zavadil, *J. Luminescence*, **2017**, *192*, 1104–1109.
32. H. Akazawa and H. Shinojima, *J. Appl. Phys.*, **2017**, *122*, 195304/1–195304/10.
33. J. G. Mao, J. Z. Ni, S. B. Wang, T. C. W. Mak and H. J. Zhang, *Polyhedron*, **1998**, *17*, 3999–4009.
34. F. H. Zhang, Y. Y. Wang, C. Lv, Y. C. Li and X. Q. Zhao, *J. Luminescence*, **2019**, *207*, 561–570.

M. A. S. Goher and F. A. Mautner *J. Molecul. Struct.*, **2007**, *846*, 153–156.